Please cite this article in press as: Wasilewski et al., Optic Atrophy 1-Dependent Mitochondrial Remodeling Controls Steroidogenesis in Trophoblasts, Current Biology (2012), doi:10.1016/j.cub.2012.04.054

Current Biology 22, 1–7, July 10, 2012 ©2012 Elsevier Ltd All rights reserved DOI 10.1016/j.cub.2012.04.054

Report

Optic Atrophy 1-Dependent Mitochondrial Remodeling Controls Steroidogenesis in Trophoblasts

Michał Wasilewski,[1] Martina Semenzato,[1] Susanne M. Rafelski,[2,6] Jennifer Robbins,[3] Anna I. Bakardjiev,[4] and Luca Scorrano[1,5,*]

[1]Dulbecco-Telethon Institute, Venetian Institute of Molecular Medicine, 35129 Padova, Italy

[2]Department of Biochemistry & Biophysics, University of California, San Francisco, San Francisco, CA 94158, USA

[3]Department of Biology, Xavier University, Cincinnati, OH 45207, USA

[4]Department of Pediatrics, University of California, San Francisco, San Francisco, CA 94143, USA

[5]Department of Cell Physiology and Medicine, University of Geneva, 1206 Geneve, Switzerland

Summary

During human pregnancy, placental trophoblasts differentiate and syncytialize into syncytiotrophoblasts that sustain progesterone production [1]. This process is accompanied by mitochondrial fragmentation and cristae remodeling [2], two facets of mitochondrial apoptosis, whose molecular mechanisms and functional consequences on steroidogenesis are unclear. Here we show that the mitochondria-shaping protein Optic atrophy 1 (Opa1) controls efficiency of steroidogenesis. During syncytialization of trophoblast BeWo cells, levels of the profission mitochondria-shaping protein Drp1 increase, and those of Opa1 and mitofusin (Mfn) decrease, leading to mitochondrial fragmentation and cristae remodeling. Manipulation of the levels of Opa1 reveal an inverse relationship with the efficiency of steroidogenesis in trophoblasts and in mouse embryonic fibroblasts where the mitochondrial steroidogenetic pathway has been engineered. In an in vitro assay, accumulation of cholesterol is facilitated in the inner membrane of isolated mitochondria lacking Opa1. Thus, Opa1-dependent inner membrane remodeling controls efficiency of steroidogenesis.

Results and Discussion

Steroidogenesis gives rise to multiple lipid hormones, which influence gestation (progesterone), sexual characters (androgens and estrogens), ion homeostasis (mineralocorticoids), and stress response (glucocorticoids) [3]. All steroidogenic pathways begin in the inner mitochondrial membrane (IMM) where cytochrome $p450_{scc}$ (Cyp11a1) transforms cholesterol to pregnenolone [4]. The steroidogenic acute regulatory protein (Star) transports cholesterol to the IMM, allowing the initiation of steroidogenesis with the remarkable exception of human placenta, where Star is not expressed. In syncytiotrophoblast, the steroidogenic cells of human placenta, progesterone synthesis coincides with structural mitochondrial changes that could facilitate cholesterol diffusion to the IMM [2]. We therefore set out to address whether and how the mitochondria-shaping machinery influences steroidogenesis.

Mitochondria Remodel during Syncytialization of Cytotrophoblasts

The human cytotrophoblast BeWo cell line, upon cyclic AMP level increase triggered by the adenylyl cyclase activator forskolin (Frk), can differentiate to syncytiotrophoblast, recapitulating the in vivo differentiation of villous trophoblast [5]. BeWo cells indeed formed multinucleated syncytia when treated with Frk, as revealed by immunostaining for the cell junction marker E-cadherin (Figure 1A). This morphological signature of differentiation was accompanied by a progressive increase in the secretion of the key syncytiotrophoblast pregnancy hormone human chorionic gonadotropin (hCG) [1] (Figure 1B), confirming the suitability of BeWo cells as a model of syncytiotrophoblasts differentiation.

During syncytiotrophoblast formation, mitochondria undergo structural changes that we wished to verify in our cellular model. Confocal imaging of undifferentiated BeWo cells engineered to stably express a yellow fluorescent protein targeted to mitochondria (mtYFP; BeWo-mtYFP) showed elongated mitochondria. Syncytialization and differentiation induced by Frk resulted in mitochondrial fragmentation with the appearance of punctuate, round-shaped organelles (Figures 1C and 1D). Electron microscopy (EM) further elucidated that these morphological changes were accompanied by the appearance of more electron-transparent matrix and by the close apposition of the inner to the outer mitochondrial membrane (OMM) (Figure 1E). A morphometric analysis confirmed that in syncytialized BeWo the number of cristae per mitochondrion was reduced by ~20% (Figure 1F). Z stacks of confocal images of mitochondrial morphology in explants from human second trimester placentas stained with the supravital mitochondrial fluorescent dye nonyl acridine orange indicated a similar elongated to fragmented transition in cyto versus syncytiotrophoblasts in vivo (Figure 1G; overall imaging of villi in 1H).

In order to address the molecular mechanism responsible for the observed fragmentation and reduction in cristae number, we interrogated the levels of the core mitochondria-shaping proteins. In mammals, fission is accomplished by dynamin related protein 1 (Drp1), which oligomerizes on mitochondria and constricts them [6]. Outer membrane (OMM) mitofusin (Mfn) 1 and 2 control mitochondrial fusion [7, 8] together with Optic atrophy 1 (Opa1), an IMM protein that also governs shape of the cristae [9, 10]. In differentiated BeWo cells that express cytochrome Cyp11a1, levels of Opa1 and Mfn2 were greatly decreased, whereas Mfn1 was less reduced and Drp1 was increased ~4-fold. Notably, levels of the respiratory chain component CoxIV and of the OMM protein Fis1 remained stable, indicating a stable mitochondrial mass during differentiation (Figures 1I and 1J). Thus, mitochondria fragment and levels of the mitochondria-shaping proteins change during differentiation from cyto to syncytiotrophoblasts in vitro and in vivo.

[6]Present address: Department of Developmental and Cell Biology, University of California, Irvine, Irvine, CA 92697, USA

*Correspondence: luca.scorrano@unige.ch

Please cite this article in press as: Wasilewski et al., Optic Atrophy 1-Dependent Mitochondrial Remodeling Controls Steroidogenesis in Trophoblasts, Current Biology (2012), doi:10.1016/j.cub.2012.04.054

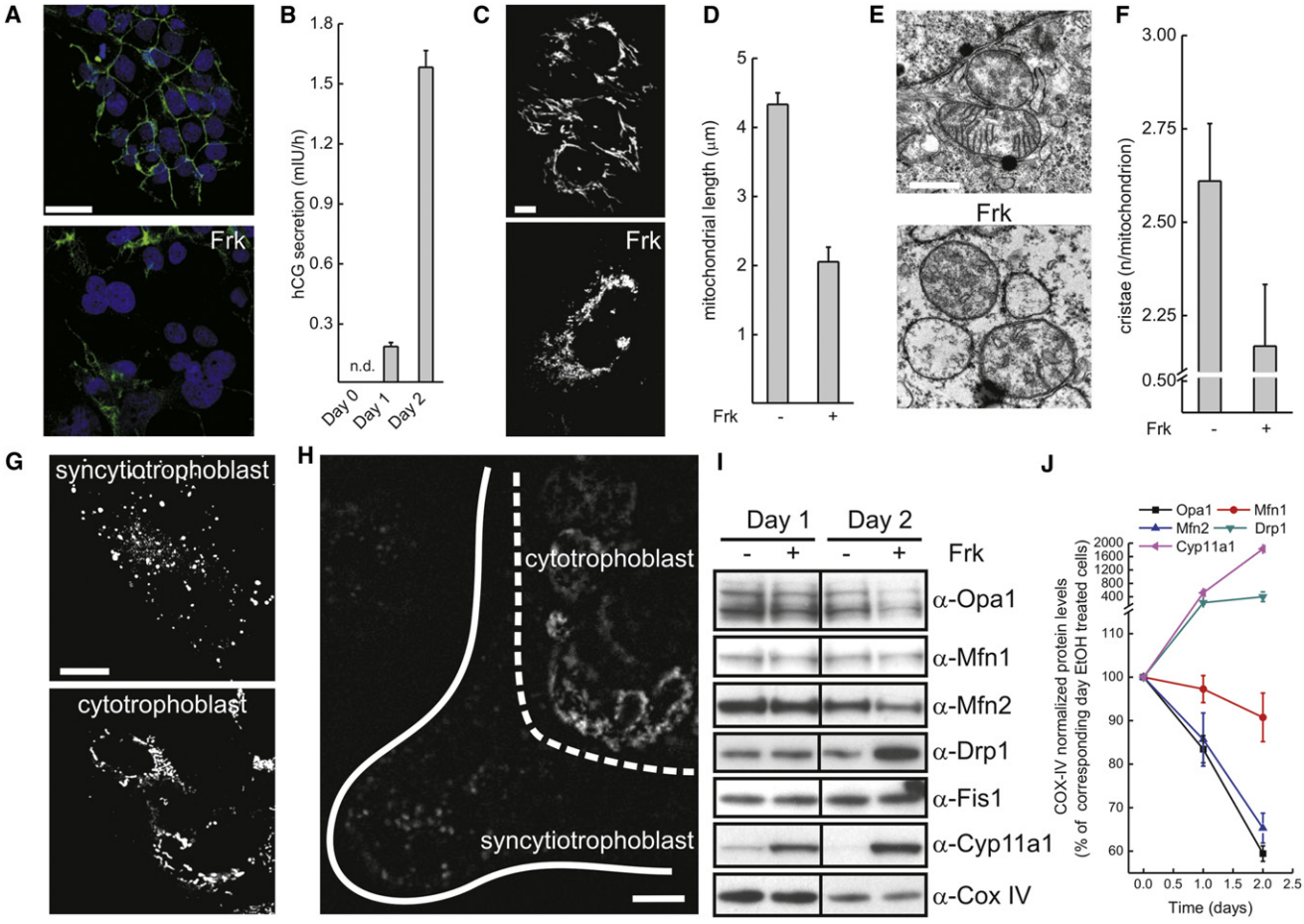

Figure 1. Remodeling of Mitochondria during Syncytialization of Trophoblasts In Vitro and In Vivo

(A) Representative confocal images of BeWo cells stained with Hoechst (blue) and anti-E-cadherin (green). Where indicated, cells were treated with Frk for 48 hr. Scale bar represents 40 μm.

(B) Secretion of hCG during differentiation of BeWo cells. Cells were treated with Frk for the indicated time and the concentration of hCG in the culture media was measured as described in Supplemental Experimental Procedures. Data represent mean ± SEM of four independent experiments. n.d., not detected.

(C) Representative confocal images of BeWo cells stably expressing mtYFP (BeWo-mtYFP). Where indicated, cells were treated with Frk for 48 hr. Scale bar represents 20 μm.

(D) Morphometric analysis of mitochondrial length in differentiating BeWo-mtYFP cells. Experiments were as in (C). Data represent mean ± SEM of six independent experiments.

(E) Representative randomly selected electron micrographs of BeWo cells. Where indicated cells were treated with Frk for 48 hr. Scale bar represents 1 μm.

(F) Morphometric analysis of mitochondrial cristae in differentiating BeWo cells. Experiments were as in (E). Data represent mean ± SEM of four independent experiments (100 mitochondria per experiment).

(G) Representative confocal images of trophoblast of human placenta (20th week of gestation) stained with nonyl acridine orange as described in Supplemental Experimental Procedures. Scale bar represents 10 μm.

(H) Confocal image of a section of human placenta (15th week of gestation) stained with MitoTracker as described in Supplemental Experimental Procedures. The dashed line indicates the border between cytotrophoblasts and syncytiotrophoblasts. The solid line indicates the surface of the chorionic villus. Scale bar represents 10 μm.

(I) Levels of mitochondria-shaping proteins during differentiation of BeWo cells. Where indicated, cells were treated with Frk for the indicated times and then lysed. Equal amounts of proteins (20 μg) were separated by SDS-PAGE and immunoblotted with the indicated antibodies.

(J) Quantification of (I). Data have been normalized to the levels of Cox IV for the corresponding day and represent mean ± SEM of three independent experiments.

Increased Availability of Cholesterol for Mitochondrial Pregnenolone Biosynthesis in Syncytiotrophoblasts

During syncytialization, we also measured an increase in the release of pregnenolone (Figure 2A), which was synthesized by Cyp11a1 as confirmed by the specific inhibitor aminoglutethimide (Figure 2B). Steroidogenesis might be influenced not only by the expression of the key steroidogenetic enzymes but also by the delivery of cholesterol to the IMM where Cyp11a1 is located. To verify this possibility, we compared the *basal* rate of pregnenolone synthesis with the *maximal* one, obtained by feeding cells with the membrane-permeable analog of cholesterol and Cyp11a1 substrate 22(R)-hydroxycholesterol (HCH) that freely diffuses to the IMM [11]. The maximal rate depends therefore only on Cyp11a1 levels, whereas the basal one reflects both Cyp11a1 levels and delivery of cholesterol to the IMM. When we fed undifferentiated BeWo cells with HCH, pregnenolone production increased approximately 15-fold, indicating that the ability

Please cite this article in press as: Wasilewski et al., Optic Atrophy 1-Dependent Mitochondrial Remodeling Controls Steroidogenesis in Trophoblasts, Current Biology (2012), doi:10.1016/j.cub.2012.04.054

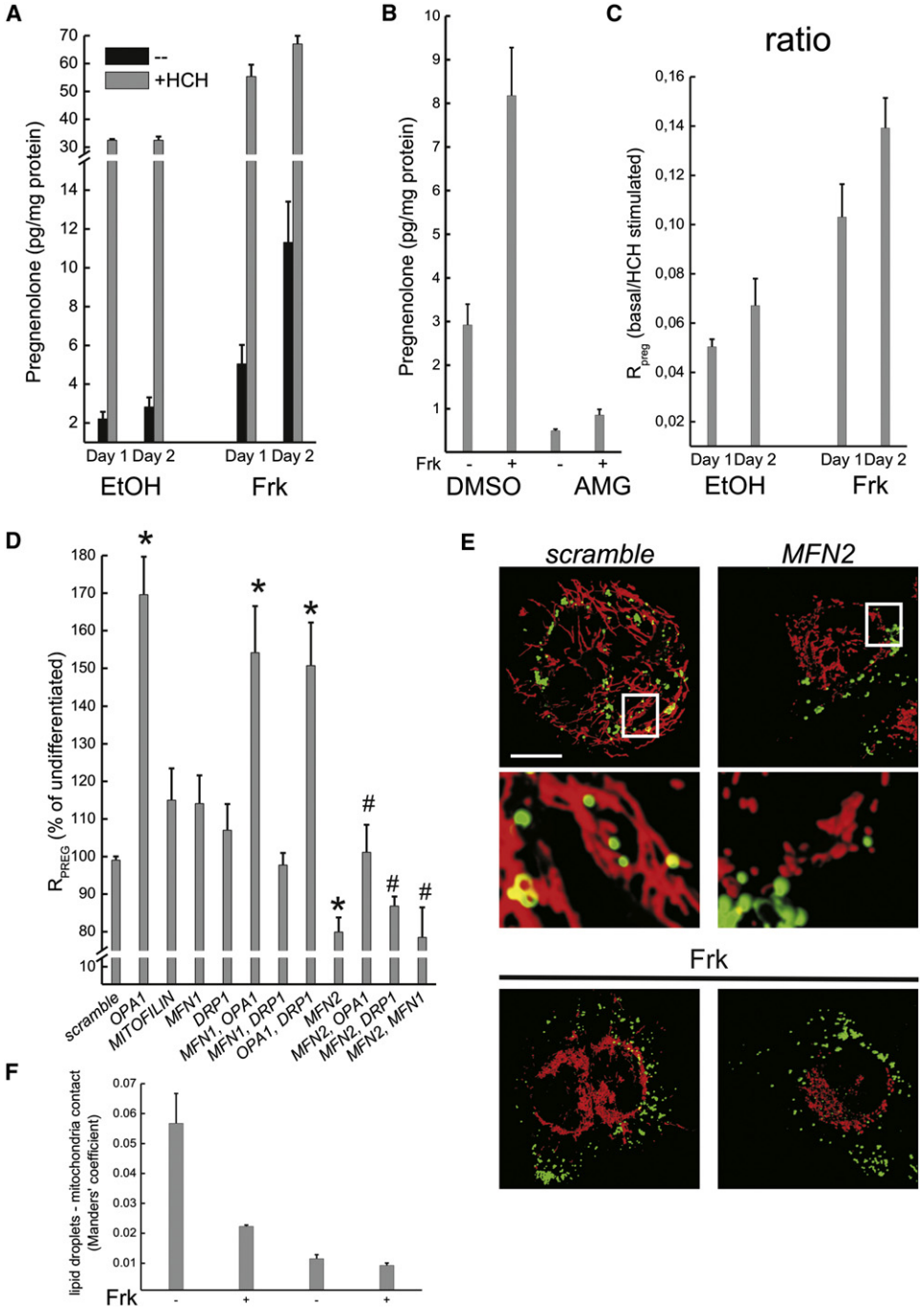

Figure 2. Genetic Analysis of the Role of Mitochondria-Shaping Proteins in Efficiency of Pregnenolone Production during Differentiation of BeWo Cells

(A) Secretion of pregnenolone was measured at the indicated times from cells treated as shown. Where indicated, cells were fed with 22(R)-hydroxycholesterol (HCH). Data represent mean ± SEM of four independent experiments.

(B) Cells were treated with ethanol or Frk for 2 days. Where indicated, 2 hr before the collection of medium for pregnenolone measurements, cells were pretreated with DL-aminoglutethimide (AMG, 1 mM). Data represent mean ± SEM of three independent experiments.

(C) The ratio between basal and maximal pregnenolone synthesis (R_{preg}) determined as in (A) was calculated. Data represent mean ± SEM of four independent experiments.

(D) R_{preg} was determined in BeWo cells transfected as indicated and treated where indicated with Frk for 48 hr. Data represent mean ± SEM of seven independent experiments. *$p < 0.05$ in a two-tailed Student's t test between scramble and single siRNA; #$p < 0.05$ in a two-tailed Student's t test between double siRNA against Mfn2 plus the indicated mitochondria-shaping protein and the corresponding single siRNA.

(E) Three-dimensional reconstructions of stacks of confocal images of lipid droplets (green) and mitochondria (red) in BeWo cells transfected with the siRNA against the indicated gene. Insets have been magnified 9×. Where indicated, cells have been treated for 2 days with Frk. Scale bar represents 20 μm.

(F) Quantification of interaction data from (E). Data represent mean ± SEM of four independent experiments.

See also Figures S1–S3.

Please cite this article in press as: Wasilewski et al., Optic Atrophy 1-Dependent Mitochondrial Remodeling Controls Steroidogenesis in Trophoblasts, Current Biology (2012), doi:10.1016/j.cub.2012.04.054

of cholesterol to reach the IMM (where Cyp11a1 is located) is a rate limiting step in pregnenolone synthesis. Upon Frk-induced differentiation, HCH-stimulated pregnenolone production was doubled (Figure 2A), indicating that the measured induction in Cyp11a1 (Figures 1I and 1J) accounts for a 2-fold increase in the production of pregnenolone. We next moved to the analysis of pregnenolone production by BeWo cells in the absence of exogenous permeable cholesterol. Released pregnenolone levels increased up to 6-fold upon differentiation (Figure 2A). Together with the HCH experiment, these results suggest that differentiation not only induces the expression of the pregnenolone biosynthetic enzymes (Figures 1I and 1J) but also (and perhaps principally) increases IMM cholesterol availability. Accordingly, the ratio between basal and maximal pregnenolone production (R_{preg}) tripled during differentiation (Figure 2C). In conclusion, the increased steroidogenetic ability of syncytiotrophoblasts is accompanied by an increase in R_{preg} that could reflect the increased cholesterol trafficking to the IMM.

Levels of OPA1 Influence Mitochondrial Pregnenolone Biosynthesis

To address whether the mitochondrial shape changes observed during differentiation of BeWo cells were causally linked to pregnenolone synthesis, we efficiently silenced Opa1, Mfn1, Mfn2, Drp1, and the cristae junction regulator mitofilin, and we overexpressed low levels of wild-type murine isoform 1 OPA1 (WT), constitutively active disassembly-resistant Q297V [12, 13], and inactive R905stop mutants of OPA1 [9] (Figures S1A–S1C available online). As expected, silencing of profusion proteins caused nonadditive mitochondrial fragmentation at steady state that could not be further aggravated by differentiation, whereas silencing of Drp1 resulted in elongation that was partially retained upon Frk treatment but abolished by the simultaneous silencing of Opa1 (Figures S1D and S1E). Expression of WT and Q297V OPA1 induced the expected mitochondrial elongation, whereas $OPA1^{R905stop}$ caused slight mitochondrial fragmentation (Figures S1F–S1H). Interestingly, the only two genetic manipulations that affected R_{preg} upon BeWo cells differentiation were the ablation of Opa1 (which increased it) and that of Mfn2 (which conversely reduced it) (Figure 2D). The influence of Opa1 on efficiency of pregnenolone biosynthesis was confirmed in the overexpression experiments: WT and constitutively active OPA1 decreased R_{preg}, whereas $OPA1^{R905stop}$ increased it (Figure S2). The stimulation of R_{preg} caused by the downregulation of Opa1 could not be counteracted by the simultaneous ablation of Drp1 but was fully inhibited by the cosilencing of Mfn2, which has an additional role in tethering mitochondria to the endoplasmic reticulum (ER) [14] (Figure 2D). The observed changes in R_{preg} were not secondary to an overall alteration of the differentiation program, as testified by the lack of effect of the genetic maneuvers listed above on the secretion of hCG (Figure S3).

Ablation of Mfn2 was the only treatment that per se reduced R_{preg}, suggesting a key role for this bifunctional mitochondria-shaping protein in the regulation of pregnenolone biosynthesis. Steroidogenesis is mainly fueled by cholesterol imported via low-density lipoproteins (LDL) and stored in lipid droplets, hydrophobic cytoplasmic structures covered with a single leaflet of polar lipids that originate from the ER [15] and that may therefore harbor ER proteins. In addition, ER per se participates in cholesterol trafficking and could therefore provide cholesterol for steroidogenesis. In BeWo cells, the fluorescent NBD-cholesterol analog indeed brightly labeled spots corresponding to lipid droplets, and to a lesser extent the ER (not shown). We therefore addressed whether Mfn2 was involved also in tethering of mitochondria to lipid droplets by analyzing pseudo-colocalization of mitochondria labeled with Mitotracker Red and lipid droplets labeled with BODIPY 493/503. Under basal conditions we observed limited contacts between mitochondria and lipid droplets, which were significantly reduced upon differentiation when levels of Mfn2 decline. Interestingly, ablation of Mfn2 almost completely abolished juxtaposition between mitochondria and lipid droplets to a level that could not be further diminished by Frk (Figures 2E and 2F). Taken together these data suggest a role for Mfn2 in lipid droplet-mitochondria contact, although it is not clear whether this contact could contribute efficiently to steroidogenesis because of its low frequency. Interestingly, defects in ER-mitochondria lipid transports had been indeed suggested in $Mfn2^{-/-}$ MEFs [16] and mice lacking MFN2 display a placental defect [17]. Our results could offer a molecular explanation to this placental deficiency: the decreased tethering between ER or lipid droplets and mitochondria in $Mfn2^{-/-}$ trophoblasts could impair progesterone biosynthesis that is particularly crucial during midgestation in rodents [18].

The combination of the genetic approaches listed here indicates that Opa1 influences pregnenolone biosynthesis, pointing to a role for cristae shape. Indeed, during differentiation of BeWo cells, the IMM remodels ([2] and Figure 1), similar to the loss of cristae observed in syncytiotrophoblasts [2, 19].

Engineered Pregnenolone Biosynthesis Is More Efficient in Mouse Embryonic Fibroblasts Lacking *Opa1*

In order to corroborate the genetic analysis performed in BeWo cells, we turned to a reductionist approach using a cellular model where we could limit the confounding variables like differentiation and syncytialization. We therefore engineered the pregnenolone biosynthetic pathway in mouse embryonic fibroblasts (MEFs) with genetically defined Opa1 expression levels. $Opa1^{-/-}$ MEFs were reconstituted by retroviral transduction with WT or with Q297V OPA1 (Figure 3A). Whereas $Opa1^{-/-}$ mitochondria were fragmented and displayed fewer cristae than their WT counterparts, reintroduction of WT OPA1 completely rescued both phenotypes and $OPA1^{Q297V}$ was as expected more efficient, fully restoring mitochondrial morphology and ultrastructure even at lower expression levels (Figures 3B and 3C). Next, we efficiently expressed the key steroidogenetic factors ferredoxin 1 (Fdx1), adrenodoxin reductase (Adxr), and cytochrome Cyp11a1 to comparable levels in WT, $Opa1^{-/-}$, and reconstituted $Opa1^{-/-}$ MEFs (Figure S4A). The expression of these three enzymes was sufficient to initiate the production of pregnenolone that could be measured at comparable levels in the supernatant of MEFs fed with HCH, indicating consistent transfection efficiency between cell lines and independent experiments (Figure S4B). Measured R_{preg} was doubled in $Opa1^{-/-}$ MEFs compared to their WT counterparts and this increase was completely inhibited in $Opa1^{-/-}$ cells reconstituted with WT or Q297V OPA1 (Figure 3D). To address whether the observed increase in R_{preg} in $Opa1^{-/-}$ MEFs was a consequence of different efficiency of cholesterol transport between OMM and IMM, we maximized it by expressing Star (Figure S4C). Interestingly, Star expression equalized R_{preg} among WT, $Opa1^{-/-}$, and reconstituted $Opa1^{-/-}$ MEFs (Figure 3E). Therefore, pregnenolone biosynthesis can be enhanced by

Please cite this article in press as: Wasilewski et al., Optic Atrophy 1-Dependent Mitochondrial Remodeling Controls Steroidogenesis in Trophoblasts, Current Biology (2012), doi:10.1016/j.cub.2012.04.054

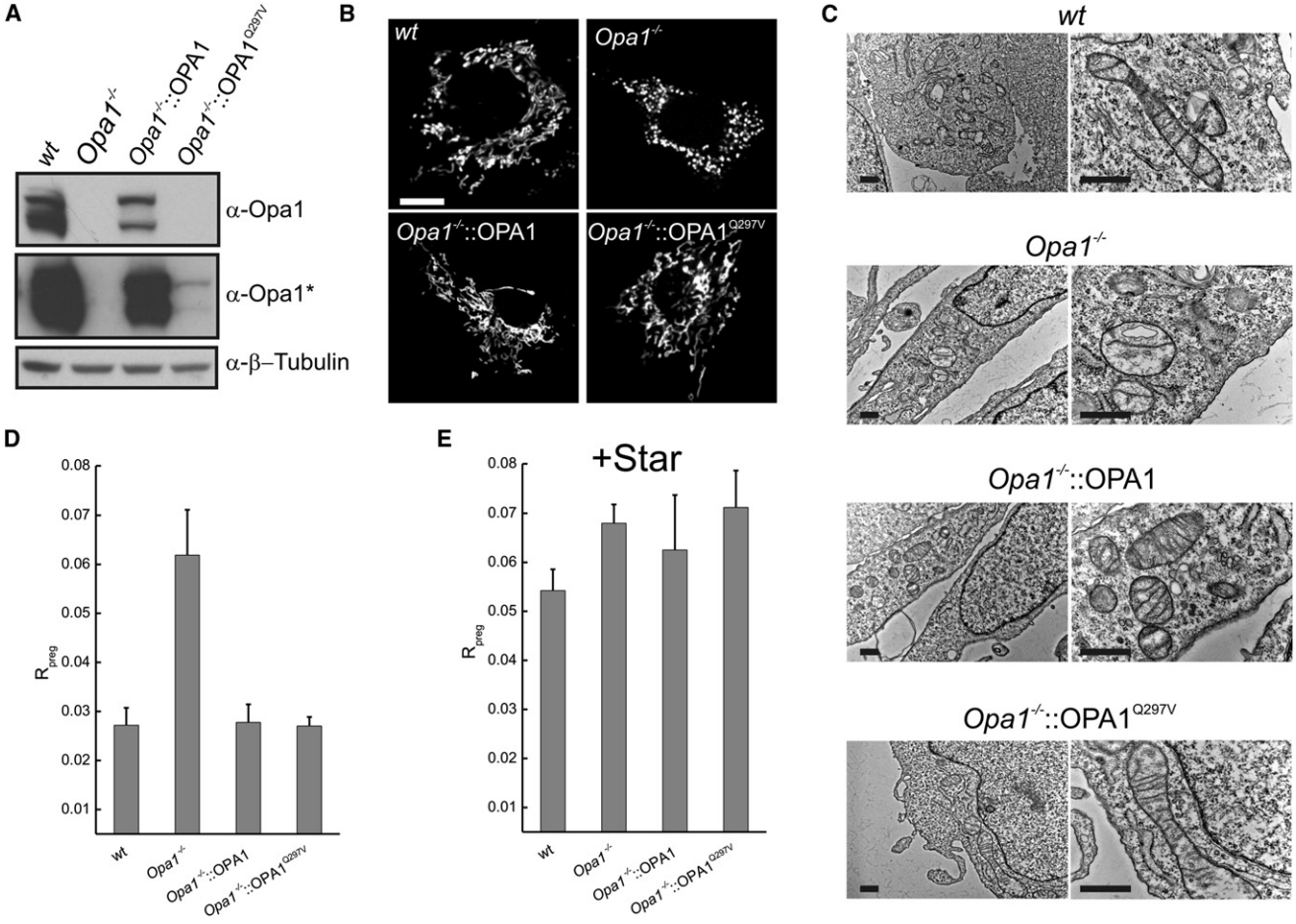

Figure 3. Efficiency of Pregnenolone Biosynthesis in Engineered MEFs Is Increased by the Absence of OPA1

(A) MEFs of the indicated genotype transduced as indicated were lysed and equal amounts of proteins (40 μg) were separated by SDS-PAGE and immunoblotted with the indicated antibodies. Asterisk denotes longer exposure time of the membrane from the panel above.

(B) Cells of the indicated genotype were transfected with mtYFP and after 24 hr, representative confocal images were acquired. Scale bar represents 20 μm.

(C) Electron micrographs of MEFs of the indicated genotype. Scale bars represent 1 μm.

(D and E) R_{preg} was determined in MEFs of the indicated genotypes 48 hr after transfection with Fdx1, Adxr, and Cyp11a11 alone (D) or in combination with Star (E). Data represent mean ± SEM of five independent experiments.

See also Figure S4.

the lack of *Opa1* to levels comparable to those achieved by the cholesterol shuttle Star in engineered nondifferentiating and nonsteroidogenic cells.

An In Vitro Assay Reveals Increased Cholesterol Loading in *Opa1*$^{-/-}$ Mitoplasts

Several factors other than an increased efficiency of cholesterol shuttling between OMM and IMM could provide the molecular basis for the higher efficiency of pregnenolone biosynthesis upon downregulation or ablation of Opa1. We therefore devised an in vitro assay to directly measure the translocation of fluorescently tagged 22-(*N*-(7-nitrobenz-2-oxa-1,3-diazol-4-yl)amino)-23,24-bisnor-5-cholen-3β-ol (NBD-cholesterol) to the IMM of isolated mitochondria (Figure 4A). Increasing concentrations of the detergent digitonin solubilized to comparable levels the OMM of *Opa1*$^{-/-}$ and *Opa1*$^{-/-}$::OPA1 mitochondria loaded with NBD-cholesterol, as revealed by the disappearance of the OMM marker TOM20 and the enrichment in the IMM marker complex III (Figure 4B). In order to verify the influence of OMM stripping on IMM structure, we turned to an assay of cytochrome c release that we successfully employed to determine the amount of cytochrome c escaping from the cristae in the intermembrane space [20]. While stripping of the OMM resulted in complete cytochrome c release from *Opa1*$^{-/-}$ mitochondria, a fraction of it was retained in *Opa1*$^{-/-}$::OPA1 mitochondria, consistent with the role of OPA1 in cristae retention of cytochrome c [10] and with the stabilization of IMM structure in *Opa1*$^{-/-}$::OPA1 mitochondria (Figure 4C). Next we compared the amount of NBD-cholesterol as determined by its fluorescence in the lipid extracts from whole mitochondria and mitoplasts. While loading of *Opa1*$^{-/-}$ and *Opa1*$^{-/-}$::OPA1 mitochondria with NBD-cholesterol was comparable, the concentration of NBD-cholesterol was higher in *Opa1*$^{-/-}$ mitoplasts (Figure 4D), suggesting that in the absence of OPA1 more cholesterol is incorporated in the IMM. This corroborates our hypothesis that OPA1 controls the flux of cholesterol to the IMM, perhaps as a consequence of the structural remodeling of the membrane. It remains unclear whether Opa1 is per se a negative regulator of cholesterol shuttling, or whether these

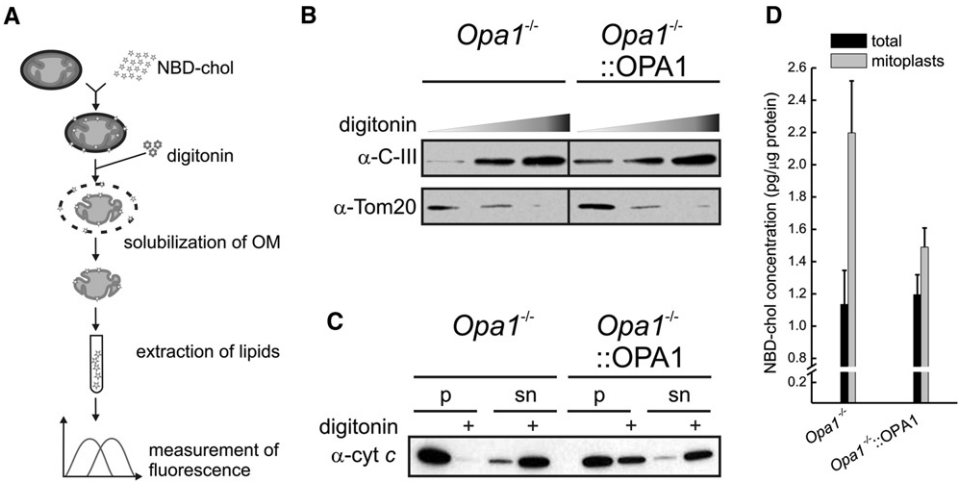

Figure 4. OPA1 Controls Loading of Cholesterol in the Inner Membrane of Purified Mitochondria

(A) A graphical outline of the experimental strategy. See Supplemental Experimental Procedures for details.

(B) Mitochondria isolated from MEFs of the indicated genotype were treated with increasing concentrations of digitonin (0, 0.72, and 0.96 mg/mg protein), sedimented by centrifugation, and lysed. Equal amounts of protein (10 μg) were separated by SDS-PAGE and immunoblotted with the indicated antibodies.

(C) The experiment was performed as in (B) (using 0.96 mg/mg protein digitonin). After centrifugation, supernatants and pellets were separated and mitoplasts were resuspended in a volume of isolation buffer equal to that of the supernatant. Equal volumes of fractions were separated by SDS-PAGE and immunoblotted for cytochrome c.

(D) Mitochondria from MEFs of the indicated genotype were treated as described in (A) and the concentration of NBD-cholesterol was determined in lipid extracts from total mitochondria and from mitoplasts. Data represent mean ± SEM of four independent experiments.

changes reflect the structural rearrangements of the IMM controlled by Opa1. Ablation of Opa1 could override the segregation of membrane proteins between the boundary inner membrane and cristae [21–23]. Interestingly, adrenal Cyp11a1 localizes to cristae [22]: it is tempting to speculate that in trophoblasts Cyp11a1 could be exposed to the OMM upon Opa1-controlled cristae remodeling.

Conclusions

Our data extend the involvement of mitochondria-shaping proteins beyond cell death, autophagy, spine plasticity, and cell migration to steroidogenesis. This novel pathway based on the delivery of cholesterol to mitochondria and to its transport to the IMM acts in parallel to Star and can substitute it in tissues when it is not expressed, like placenta and potentially nervous system, where Star involvement in the synthesis of neurosteroids is not well established [3].

Supplemental Information

Supplemental Information includes Supplemental Experimental Procedures and four figures and can be found with this article online at doi:10.1016/j.cub.2012.04.054.

Acknowledgments

L.S. is a Senior Telethon Scientist of the Dulbecco-Telethon Institute. This research was supported by Telethon Italy S02016, AIRC Italy, and Swiss National Foundation SNF 31-118171. Placenta microscopy was performed at the Nikon Imaging Center, UCSF. S.M.R. was supported by a Herbert Boyer postdoctoral fellowship. A.I.B. was supported by NIH grant R01 AI84928.

Received: December 12, 2011
Revised: March 28, 2012
Accepted: April 25, 2012
Published online: May 31, 2012

References

1. Tuckey, R.C. (2005). Progesterone synthesis by the human placenta. Placenta *26*, 273–281.
2. Martínez, F., Kiriakidou, M., and Strauss, J.F., 3rd. (1997). Structural and functional changes in mitochondria associated with trophoblast differentiation: methods to isolate enriched preparations of syncytiotrophoblast mitochondria. Endocrinology *138*, 2172–2183.
3. Miller, W.L., and Auchus, R.J. (2011). The molecular biology, biochemistry, and physiology of human steroidogenesis and its disorders. Endocr. Rev. *32*, 81–151.
4. Shikita, M., and Hall, P.F. (1973). Cytochrome P-450 from bovine adrenocortical mitochondria: an enzyme for the side chain cleavage of cholesterol. I. Purification and properties. J. Biol. Chem. *248*, 5598–5604.
5. Wice, B., Menton, D., Geuze, H., and Schwartz, A.L. (1990). Modulators of cyclic AMP metabolism induce syncytiotrophoblast formation in vitro. Exp. Cell Res. *186*, 306–316.
6. Smirnova, E., Griparic, L., Shurland, D.L., and van der Bliek, A.M. (2001). Dynamin-related protein Drp1 is required for mitochondrial division in mammalian cells. Mol. Biol. Cell *12*, 2245–2256.
7. Santel, A., Frank, S., Gaume, B., Herrler, M., Youle, R.J., and Fuller, M.T. (2003). Mitofusin-1 protein is a generally expressed mediator of mitochondrial fusion in mammalian cells. J. Cell Sci. *116*, 2763–2774.
8. Santel, A., and Fuller, M.T. (2001). Control of mitochondrial morphology by a human mitofusin. J. Cell Sci. *114*, 867–874.
9. Cipolat, S., Martins de Brito, O., Dal Zilio, B., and Scorrano, L. (2004). OPA1 requires mitofusin 1 to promote mitochondrial fusion. Proc. Natl. Acad. Sci. USA *101*, 15927–15932.
10. Frezza, C., Cipolat, S., Martins de Brito, O., Micaroni, M., Beznoussenko, G.V., Rudka, T., Bartoli, D., Polishuck, R.S., Danial, N.N., De Strooper, B., and Scorrano, L. (2006). OPA1 controls apoptotic cristae remodeling independently from mitochondrial fusion. Cell *126*, 177–189.
11. Lin, D., Sugawara, T., Strauss, J.F., 3rd, Clark, B.J., Stocco, D.M., Saenger, P., Rogol, A., and Miller, W.L. (1995). Role of steroidogenic acute regulatory protein in adrenal and gonadal steroidogenesis. Science *267*, 1828–1831.
12. Misaka, T., Miyashita, T., and Kubo, Y. (2002). Primary structure of a dynamin-related mouse mitochondrial GTPase and its distribution in brain, subcellular localization, and effect on mitochondrial morphology. J. Biol. Chem. *277*, 15834–15842.

Please cite this article in press as: Wasilewski et al., Optic Atrophy 1-Dependent Mitochondrial Remodeling Controls Steroidogenesis in Trophoblasts, Current Biology (2012), doi:10.1016/j.cub.2012.04.054

13. Yamaguchi, R., Lartigue, L., Perkins, G., Scott, R.T., Dixit, A., Kushnareva, Y., Kuwana, T., Ellisman, M.H., and Newmeyer, D.D. (2008). Opa1-mediated cristae opening is Bax/Bak and BH3 dependent, required for apoptosis, and independent of Bak oligomerization. Mol. Cell *31*, 557–569.
14. de Brito, O.M., and Scorrano, L. (2008). Mitofusin 2 tethers endoplasmic reticulum to mitochondria. Nature *456*, 605–610.
15. Walther, T.C., and Farese, R.V., Jr. (2009). The life of lipid droplets. Biochim. Biophys. Acta. *1791*, 459–466.
16. Hailey, D.W., Rambold, A.S., Satpute-Krishnan, P., Mitra, K., Sougrat, R., Kim, P.K., and Lippincott-Schwartz, J. (2010). Mitochondria supply membranes for autophagosome biogenesis during starvation. Cell *141*, 656–667.
17. Chen, H., Detmer, S.A., Ewald, A.J., Griffin, E.E., Fraser, S.E., and Chan, D.C. (2003). Mitofusins Mfn1 and Mfn2 coordinately regulate mitochondrial fusion and are essential for embryonic development. J. Cell Biol. *160*, 189–200.
18. Sher, N., and Orly, J. (2006). Analysis of trophoblast giant cell steroidogenesis in primary cultures. Methods Mol. Med. *122*, 301–319.
19. Matsubara, S., Takayama, T., Iwasaki, R., Izumi, A., Watanabe, T., and Sato, I. (2001). Chorion laeve trophoblasts of preeclamptic fetal membranes: histochemically detectable enzyme activities do not change at a subcellular level. Eur. J. Histochem. *45*, 211–217.
20. Scorrano, L., Ashiya, M., Buttle, K., Weiler, S., Oakes, S.A., Mannella, C.A., and Korsmeyer, S.J. (2002). A distinct pathway remodels mitochondrial cristae and mobilizes cytochrome c during apoptosis. Dev. Cell *2*, 55–67.
21. Ardail, D., Privat, J.P., Egret-Charlier, M., Levrat, C., Lerme, F., and Louisot, P. (1990). Mitochondrial contact sites. Lipid composition and dynamics. J. Biol. Chem. *265*, 18797–18802.
22. Cherradi, N., Rossier, M.F., Vallotton, M.B., Timberg, R., Friedberg, I., Orly, J., Wang, X.J., Stocco, D.M., and Capponi, A.M. (1997). Submitochondrial distribution of three key steroidogenic proteins (steroidogenic acute regulatory protein and cytochrome p450scc and 3beta-hydroxysteroid dehydrogenase isomerase enzymes) upon stimulation by intracellular calcium in adrenal glomerulosa cells. J. Biol. Chem. *272*, 7899–7907.
23. He, Y., Liu, J., Grossman, D., Durrant, D., Sweatman, T., Lothstein, L., Epand, R.F., Epand, R.M., and Lee, R.M. (2007). Phosphorylation of mitochondrial phospholipid scramblase 3 by protein kinase C-delta induces its activation and facilitates mitochondrial targeting of tBid. J. Cell. Biochem. *101*, 1210–1221.